The gap-tungsten-1 interatomic potential.

Wojciech J. Szlachta

ESDG
12 February 2014

Computational Modelling of Materials

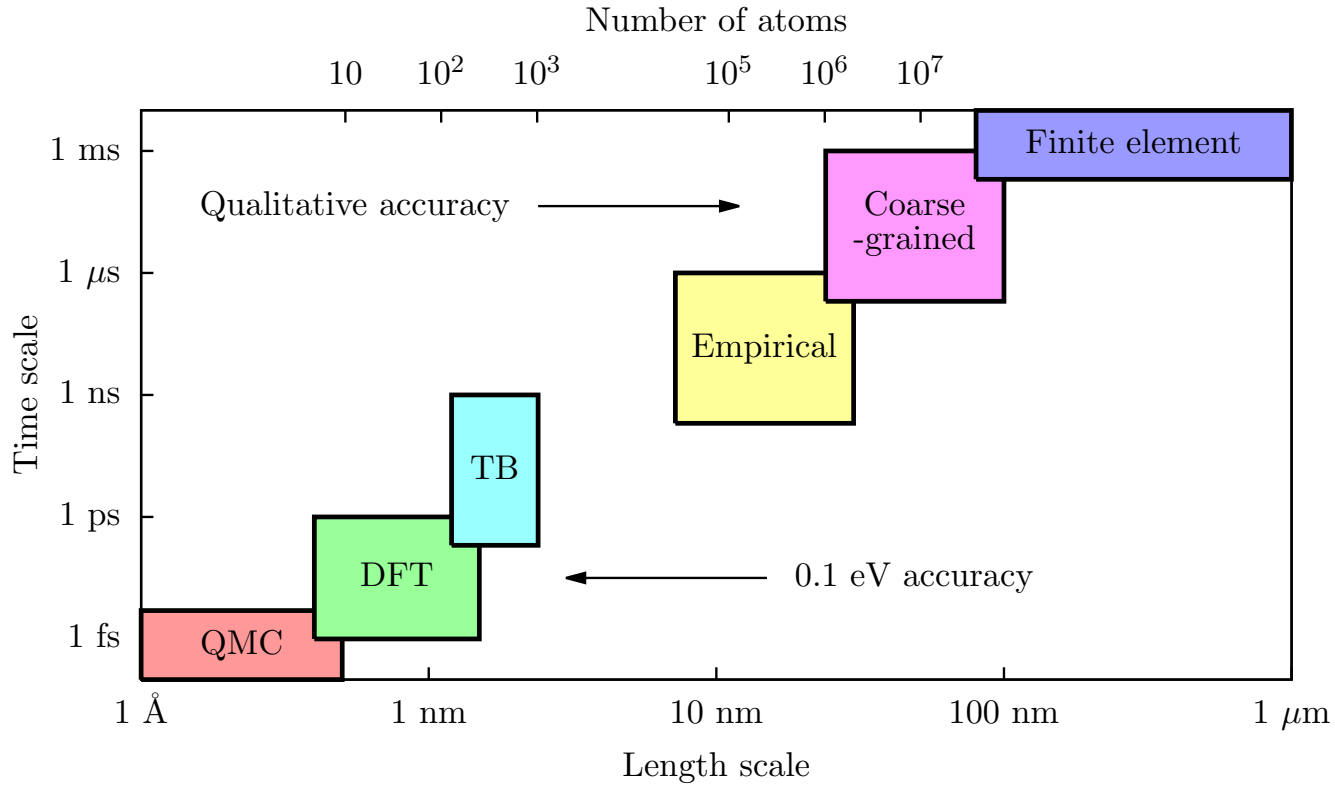

- Significant cost savings can be realized in materials design and in process optimization by using science-based computational modelling
- Calculations from first principles lead to predictive capabilities that allow discovering novel materials with desired properties

Creating Empirical Potentials

- Typical interatomic potential
  - fixed functional form with adjustable parameters (i.e. empirical, analytical formula)
  - fit fixed number of free parameters to reproduce target properties

$$E = \sum_{i}^{N} V_1(\mathbf{x}^{(i)}) + \underbrace{\sum_{i}^{N} \sum_{\substack{j \\ j<i}}^{N} V_2(\mathbf{x}^{(i)}, \mathbf{x}^{(j)})}_{\text{bonds}} + \underbrace{\sum_{i}^{N} \sum_{\substack{j \\ j<i}}^{N} \sum_{\substack{k \\ k<j}}^{N} V_3(\mathbf{x}^{(i)}, \mathbf{x}^{(j)}, \mathbf{x}^{(k)})}_{\text{angles}} + \dots$$

Lennard-Jones (LJ) Potential

$$E = \sum_{i}^{N} \epsilon_i$$

$$\epsilon_i = \sum_{j}^{N} \left(\frac{A}{r^{12}} - \frac{B}{r^{6}} \right)$$

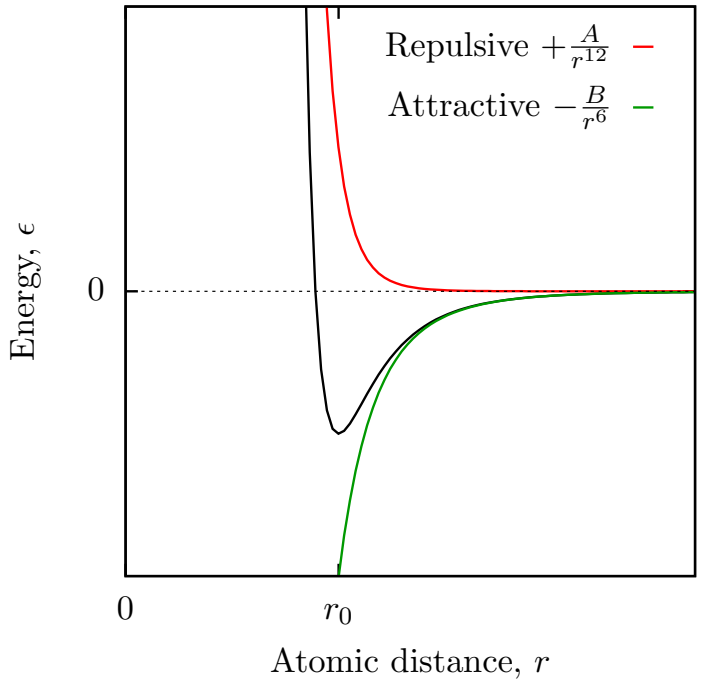

- choose target properties
- fit parameters A and B to reproduce target properties

Gaussian Process Regression

- Start with prior distribution over functions
- Set of values is observed
- Apply **Bayesian probability** / **machine learning** to infer underlying function

Bayes' theorem

$$\text{posterior} = \frac{\text{likelihood} \times \text{prior}}{\text{marginal likelihood}}$$

- Combine Gaussian prior with Gaussian likelihood function for each observed value to calculate posterior distribution for any new location

Gaussian Process Regression

- Optimal way of interpolating many-dimensional functions
- No fixed functional form
- No fixed number of free parameters

$$\epsilon_i(\mathbf{q}_i) = \sum_j \alpha_j \overbrace{k(\mathbf{q}_j, \mathbf{q}_i)}^{\text{covariance function}}$$

$$\sigma^2_{\epsilon_i}(\mathbf{q}_i) = k(\mathbf{q}_i, \mathbf{q}_i) - \sum_j \beta_j k(\mathbf{q}_j, \mathbf{q}_i)$$

Covariance function $k(\mathrm{q}_j, \mathrm{q}_i)$

Prior distribution over functions is determined by choice of the covariance function.

Gaussian Process Regression

- Optimal way of interpolating many-dimensional functions
- No fixed functional form
- No fixed number of free parameters

$$\epsilon_i(\mathbf{q}_i) = \sum_j \alpha_j \overbrace{k(\mathbf{q}_j, \mathbf{q}_i)}^{\text{covariance function}}$$

$$\sigma^2_{\epsilon_i}(\mathbf{q}_i) = k(\mathbf{q}_i, \mathbf{q}_i) - \sum_j \beta_j k(\mathbf{q}_j, \mathbf{q}_i)$$

Training data $\{\epsilon_j, \mathbf{q}_j\}_j$

Fit quality determined by both training data and choice of the covariance function.

Gaussian Process Regression

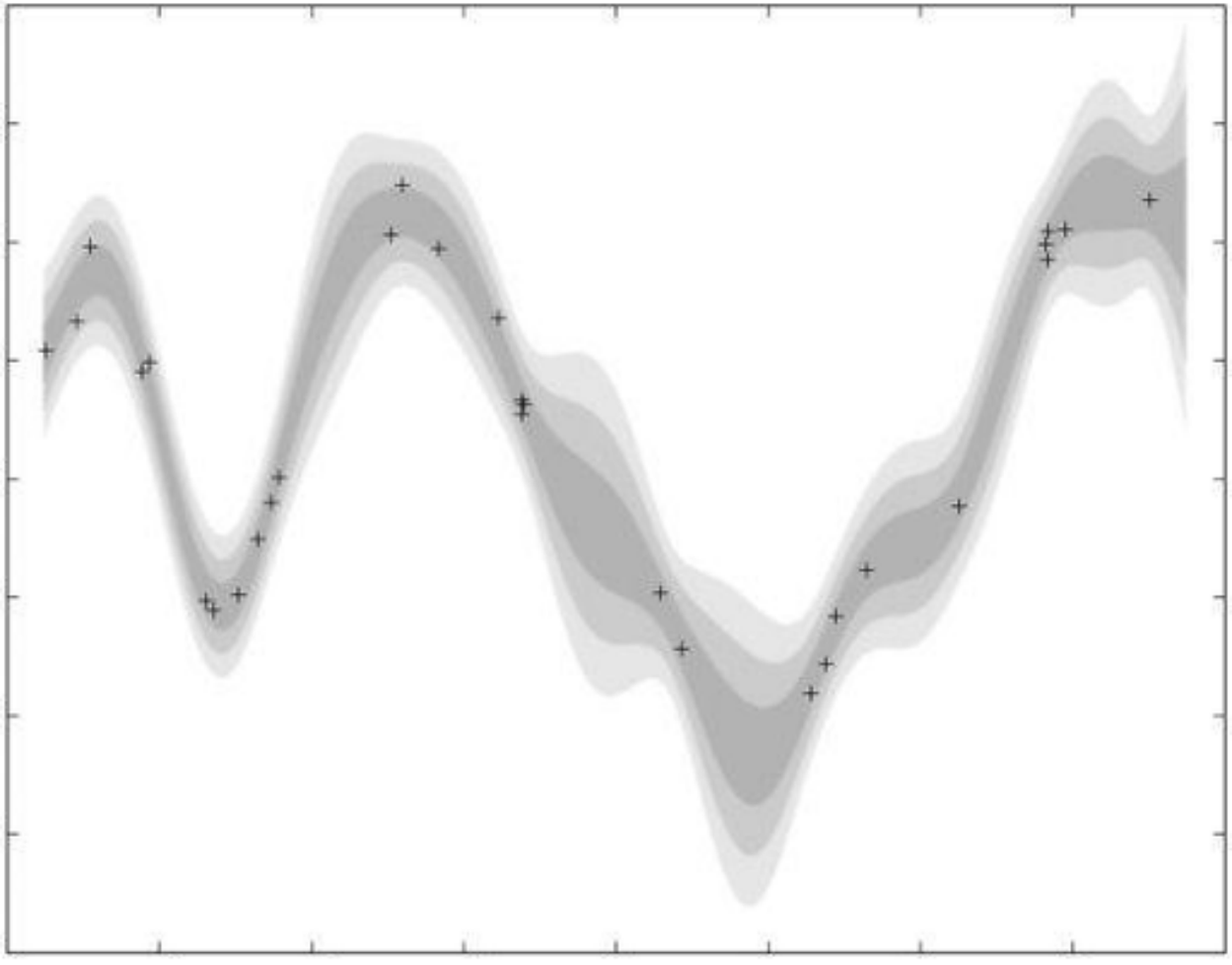

Gaussian Approximation Potential

- Compute many-body atomic energy function

$$\epsilon_i = \epsilon(\{\mathbf{x}_j - \mathbf{x}_i\}_j^N) = \epsilon(\mathbf{q}_i)$$

- Fit to arbitrary precision QM data

- **Need rotationally and permutationally invariant description of atomic environment!**

Decriptor vs. covariance function symmetries

$$\begin{array}{c} k(\mathbf{q}_j, \mathbf{q}_i) \\ + \\ \{\mathbf{x}_{k'} - \mathbf{x}_i\}_{k'} \rightarrow \mathbf{q}_i \end{array} \longleftrightarrow \begin{array}{c} k^*(\{\mathbf{x}_{k''} - \mathbf{x}_j\}_{k''}, \\ \{\mathbf{x}_{k'} - \mathbf{x}_i\}_{k'}) \end{array}$$

Gaussian Approximation Potential

Bispectrum	**Smooth Overlap of Atomic Positions**
expand atomic density using 4d spherical harmonics basis	expand atomic density using 3d spherical harmonics and radial basis
atoms represented by Dirac δ function	atoms represented by Gaussian function
square exponential covariance	dot product covariance

Gaussian Approximation Potential

- **Atomic energies cannot be directly computed from QM data!**

Training from total energies, forces and stresses

Inferring function $\epsilon(\mathbf{q}_i)$ from linear combination of its values / partial derivatives (and atomic positions) possible.

total energies: $$E = \sum_i^N \epsilon_i$$

atomic forces: $$\{\mathbf{f}^{(i)} = -\boldsymbol{\nabla}^{(i)} \sum_j^N \epsilon_j\}_i^N$$

stress virials: $$\tau_{\alpha\beta} = -\sum_i^N x_\alpha^{(i)} \frac{\partial}{\partial x_\beta^{(i)}} \sum_j^N \epsilon_j$$

- Pseudo training points to deal with large data sets efficiently (which optimally represent the underlaying teaching data)

Tungsten

- Refractory transition metal with the highest melting temperature ($3680\,\mathrm{K}$)
- Crystallized in a body-centered-cubic (BCC) structure

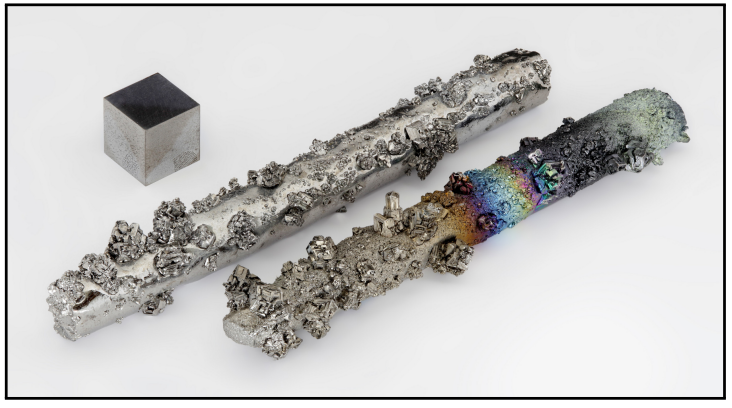

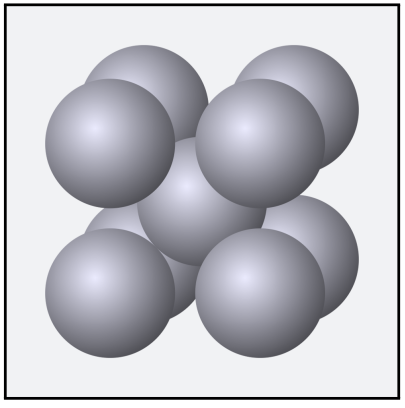

- Applications include
  - light bulb filaments, electrical contacts, welding electrodes and high-temperature furnace elements
  - tungsten might be one of the structural materials for fusion reactor ITER project

Tungsten

- Slip can occur along nearest neighbour direction $\frac{1}{2}\langle 111\rangle$ (also the shortest Burgers vector)
- The most densely packed planes of the $\langle 111\rangle$ zone are the $\{110\}$ planes

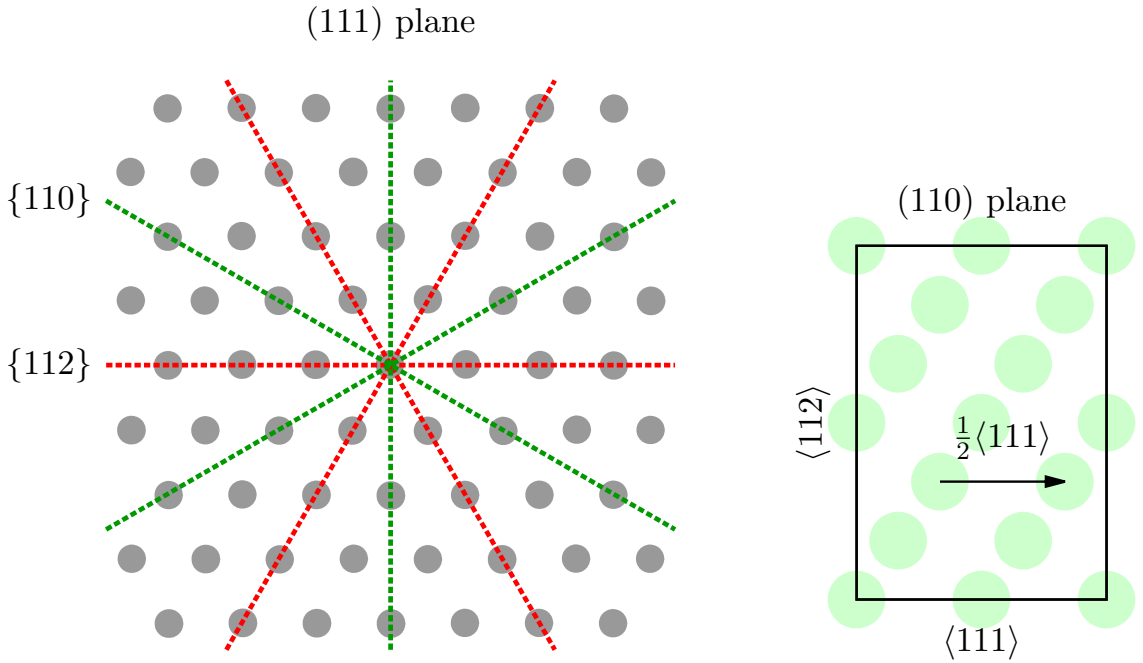

Tungsten Slip Planes

Slip plane		separation distance
$\langle 111 \rangle \{110\}$	$\rightarrow$	$\frac{1}{\sqrt{2}}\, a$
$\langle 111 \rangle \{112\}$	$\rightarrow$	$\frac{1}{\sqrt{6}}\, a$
$\langle 111 \rangle \{123\}$	$\rightarrow$	$\frac{1}{\sqrt{14}}\, a$
$\langle 111 \rangle \{134\}$	$\rightarrow$	$\frac{1}{\sqrt{26}}\, a$

Tungsten Dislocations

- Plasticity behaviour largely attributed to lattice crystallography
- Dominant dislocation type in bcc metals is $\frac{1}{2}\langle 111 \rangle$ screw
- $\langle 110 \rangle$ dislocations observed, but believed to be product of the dominant $\frac{1}{2}\langle 111 \rangle$ screw dislocations

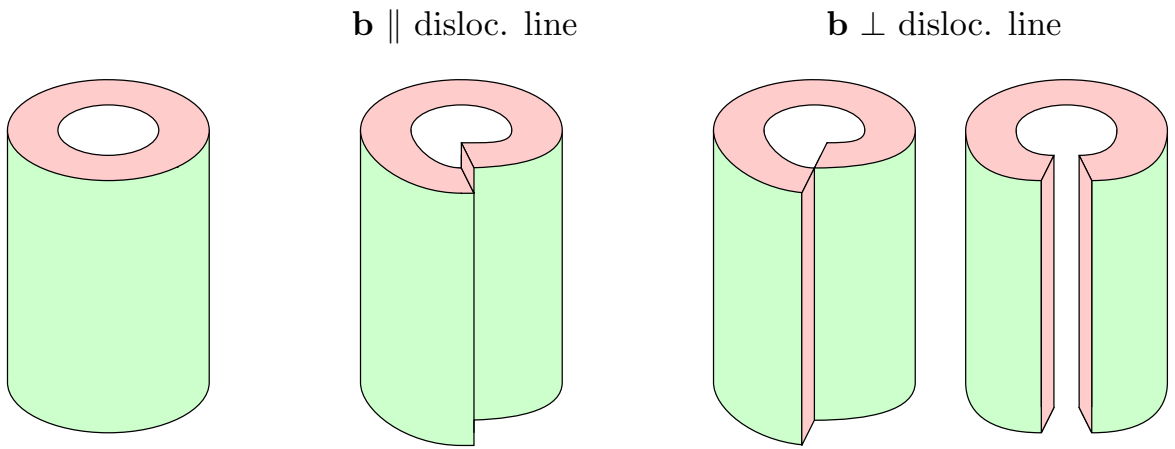

Dislocation Core

- At long range behaviour is determined by the linear elasticity theory
- Short range dislocation core structure

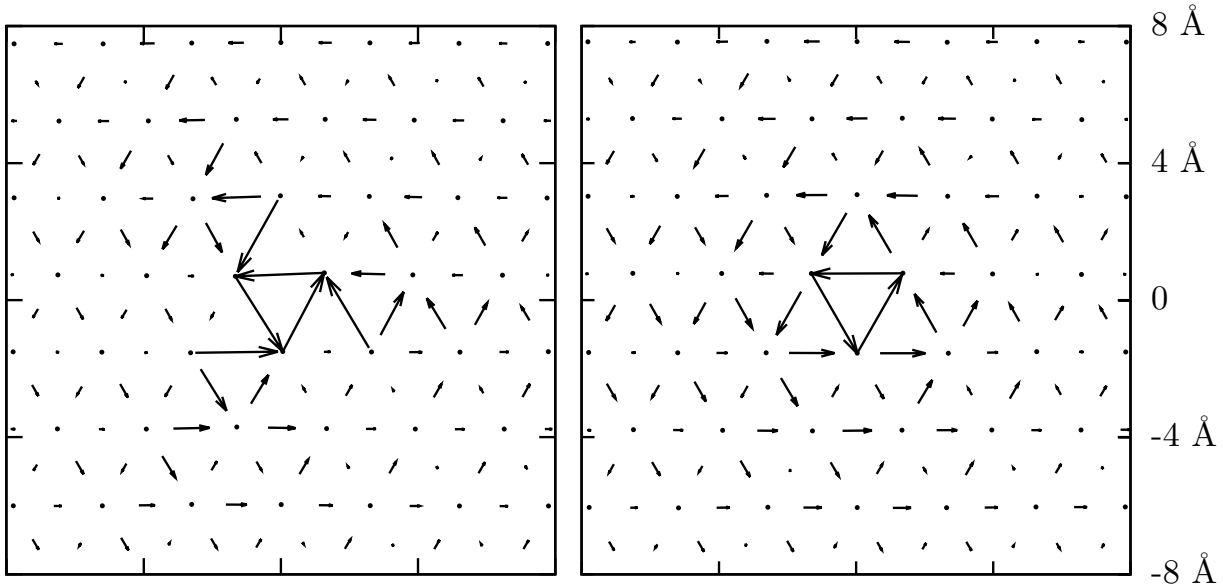

Dislocation Displacement Maps vs. Nye Tensor

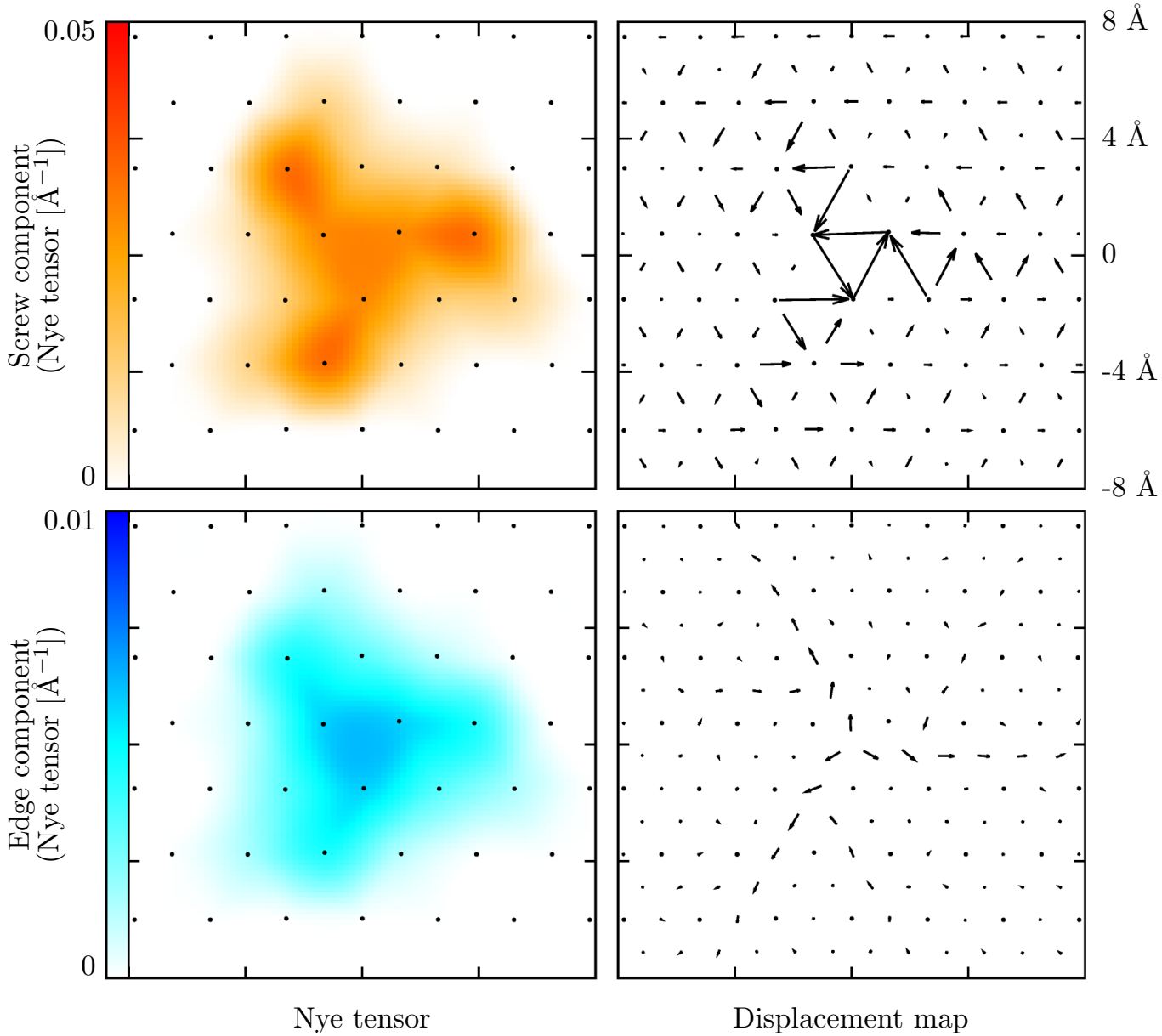

Dislocation Simulation Approaches

Dislocation Quadrupole

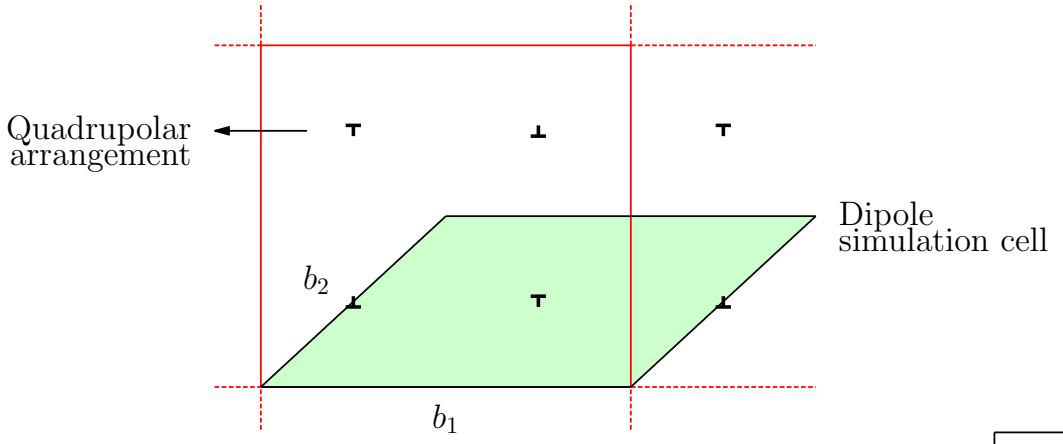

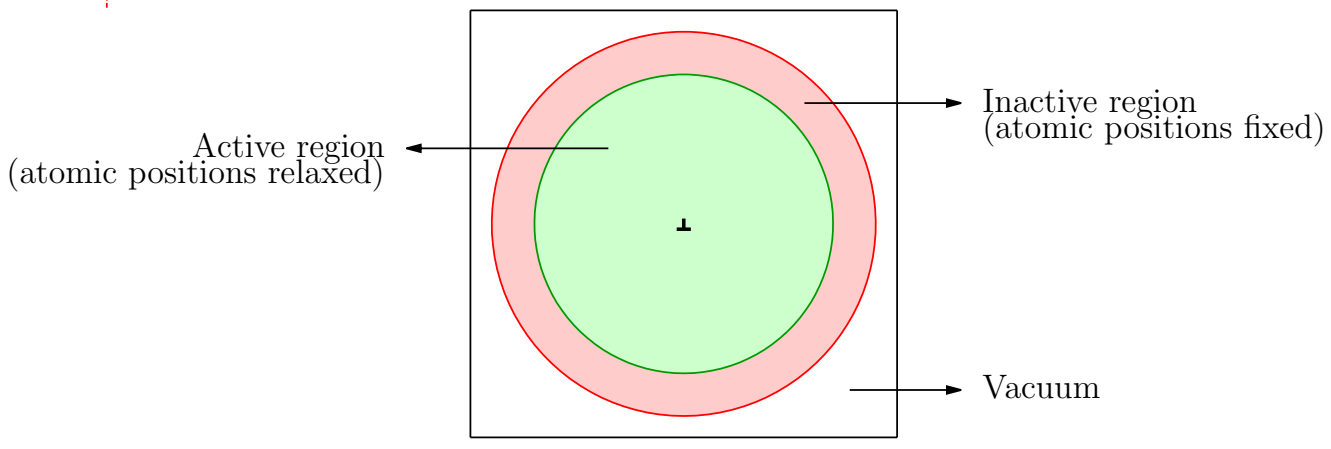

Isolated Dislocation

DFT Calculations

DFT parameters for converged energies, forces and stresses

plane-wave energy cutoff,	E_{cut}	$\rightarrow$	600	eV
k-point sampling density,	ρ	$\rightarrow$	0.015	$\mathrm{\AA}^{-1}$
smearing width,	w	$\rightarrow$	0.1	eV

GAP Recipe

1.	Elastic constants 2000 environments	$\rightarrow$	MC sampling in the lattice space temperature: $300\,\mathrm{K}$ • slice sampling algorithm • primitive unit cell
2.	Phonon spectrum 7680 environments	$\rightarrow$	MD, no defects temperature: $300, 1000\,\mathrm{K}$ volumes: ground state, $\pm 1\%$ • 128 at. simulation cell
3.	Vacancy 23740 environments	$\rightarrow$	MD, isolated monovacancy temperature: $300, 1000\,\mathrm{K}$ volumes: ground state, $\pm 1\%$ • 53 and 127 at. simulation cell
4.	Surfaces 2160 environments	$\rightarrow$	MD, (100), (110), (111), (112) temperature: $300\,\mathrm{K}$ volumes: ground state • 12 at. simulation cell
5.	Gamma surfaces 74196 environments	$\rightarrow$	MD, (110), (112) temperature: $300\,\mathrm{K}$ volumes: ground state, $\pm 1\%$ • 12 at. simulation cell

GAP Results

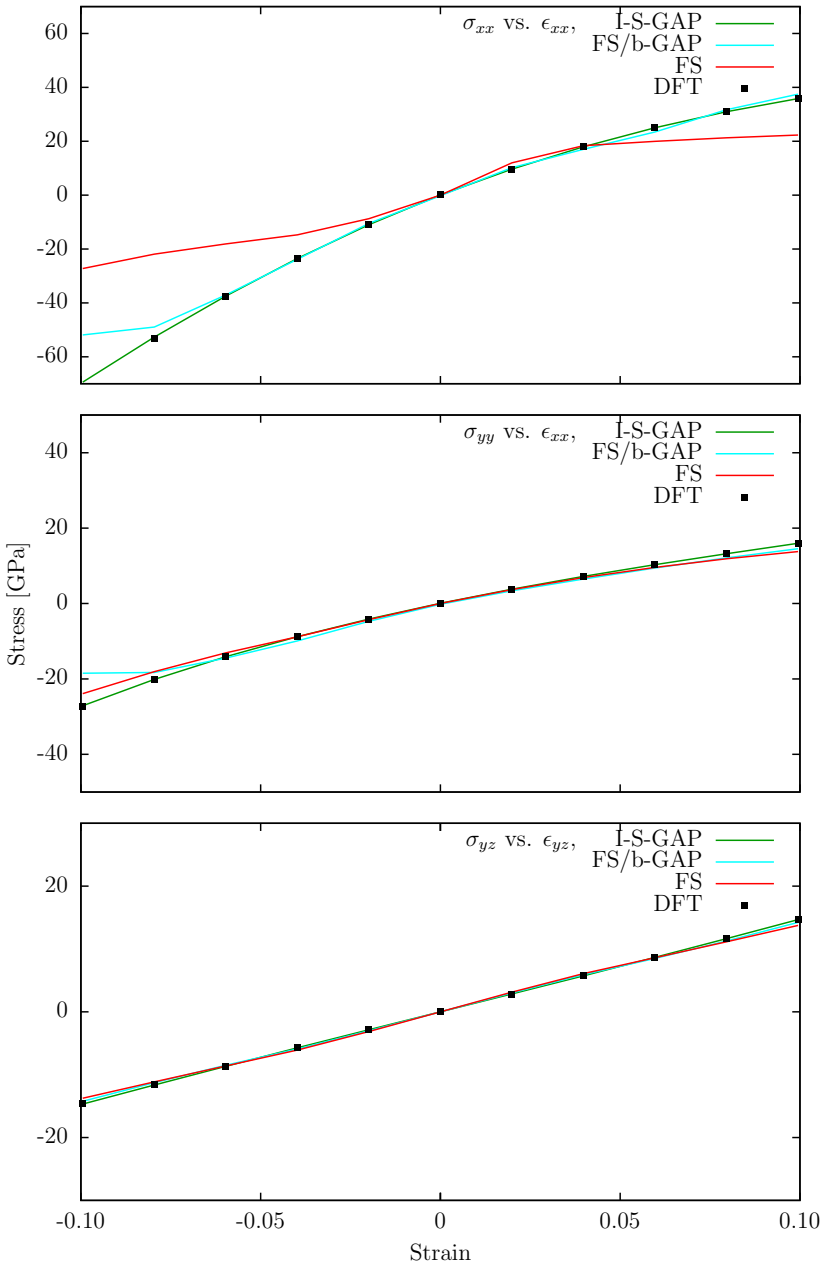
σ_{xx} vs. ϵ_{xx},
I-S-GAP
FS/b-GAP
FS
DFT
σ_{yy} vs. ϵ_{xx},
I-S-GAP
FS/b-GAP
FS
DFT
σ_{yz} vs. ϵ_{yz},
I-S-GAP
FS/b-GAP
FS
DFT
Stress [GPa]
Strain
60
40
20
0
-20
-40
-60
-0.10
-0.05
0
0.05
0.10

GAP Results

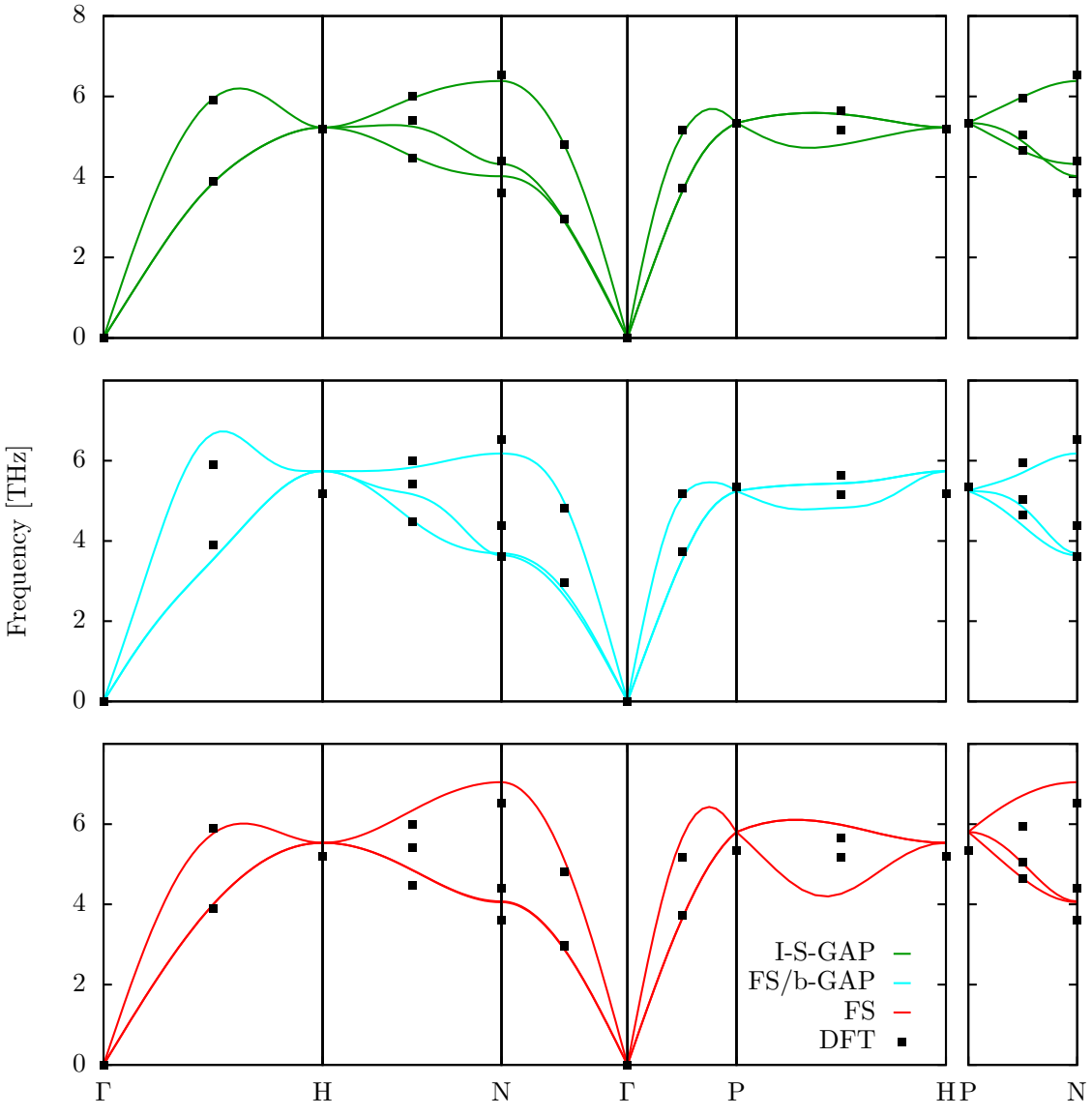

GAP Results

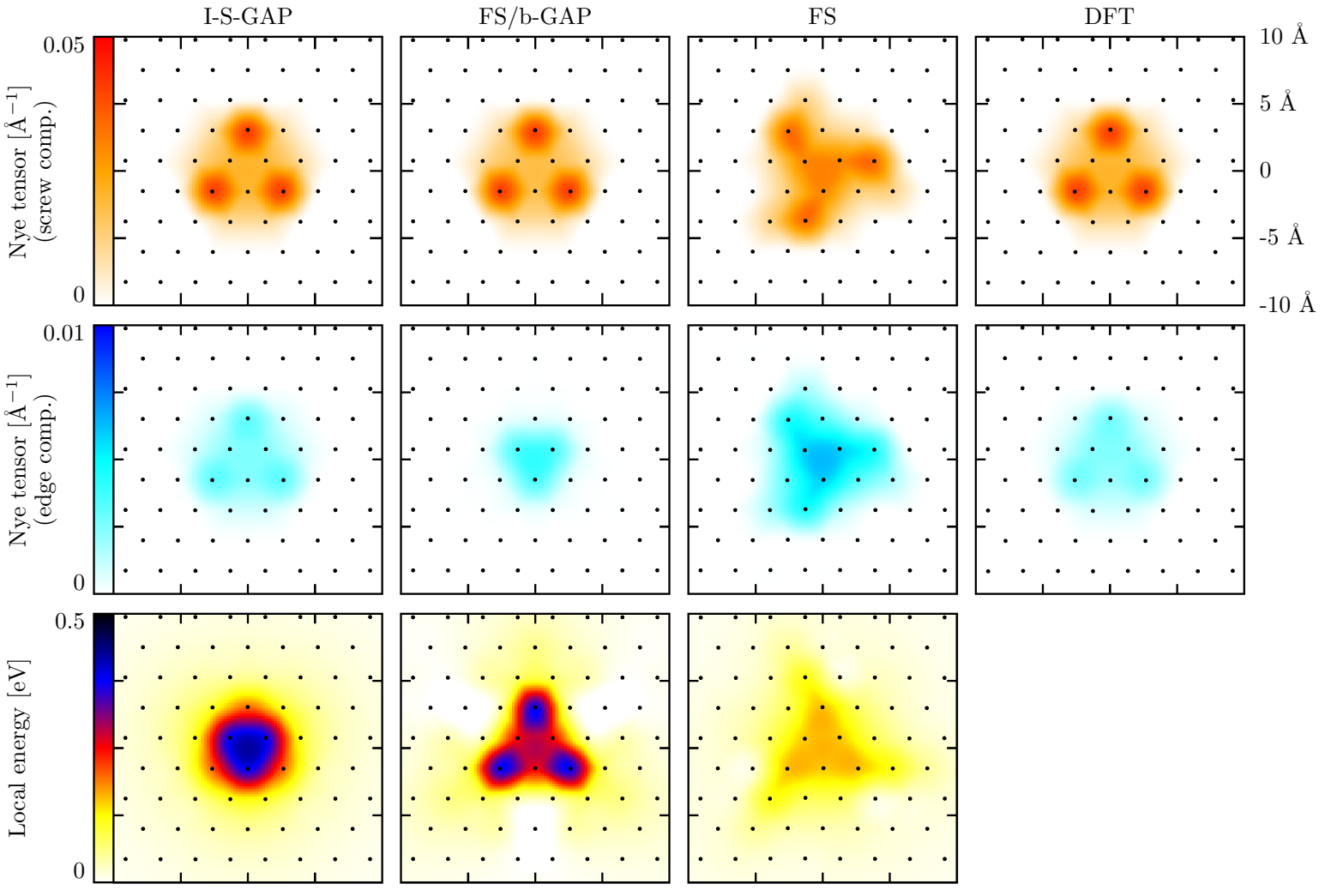
I-S-GAP
FS/b-GAP
FS
DFT
Nye tensor [Å^{-1}] (screw comp.)
0.05
0
Nye tensor [Å^{-1}] (edge comp.)
0.01
0
Local energy [eV]
0.5
0
10 Å
5 Å
0
-5 Å
-10 Å

Bispectrum vs. SOAP

- Both bispectrum and SOAP are based on expansion in spherical harmonics that needs to be truncated

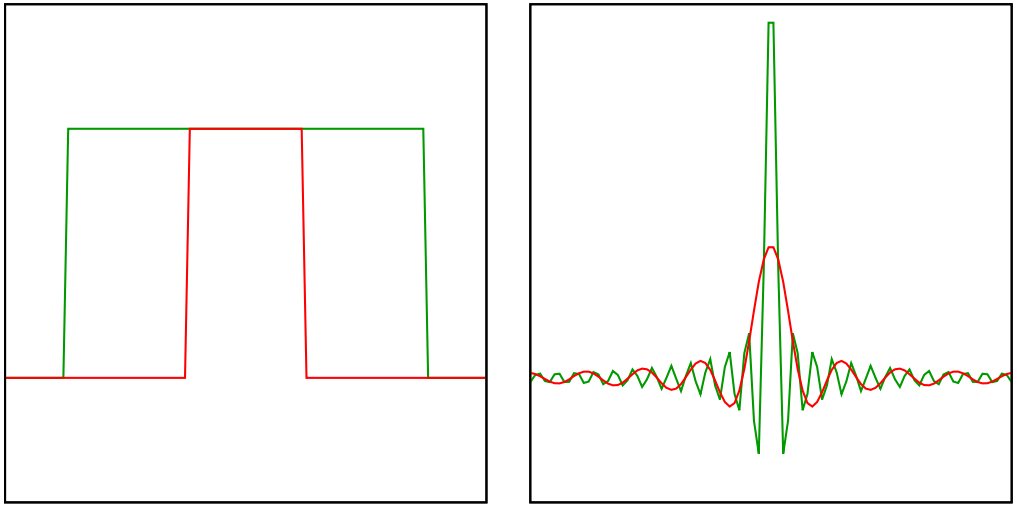

Fourier / bispectrum space | Real space

- **Failure of bispectrum based GAP is caused by the use of Dirac δ functions!**

GAP Results

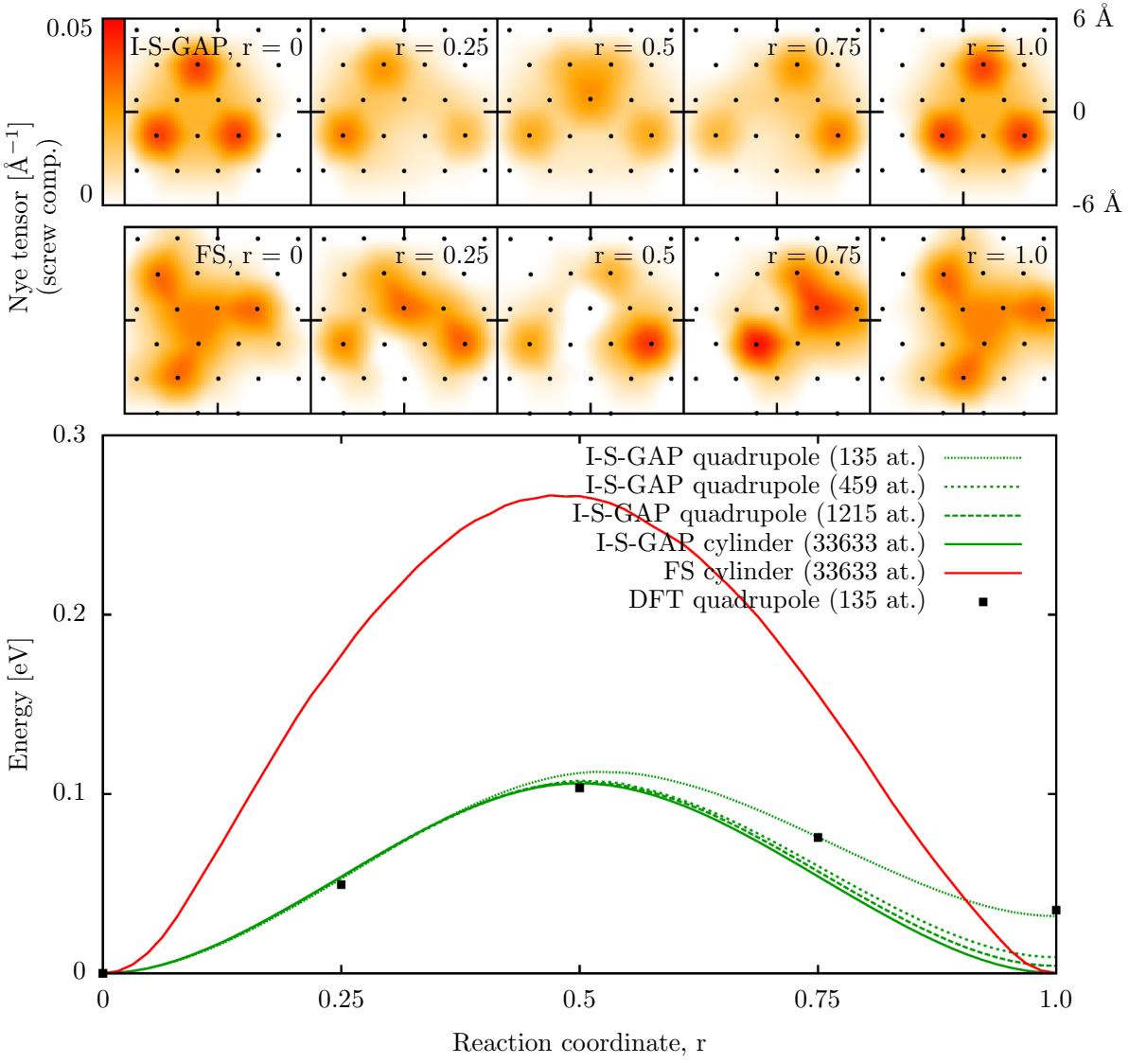
I-S-GAP, r = 0
r = 0.25
r = 0.5
r = 0.75
r = 1.0
FS, r = 0
r = 0.25
r = 0.5
r = 0.75
r = 1.0
0.05
0
6 Å
0
-6 Å
Nye tensor [Å^{-1}]
(screw comp.)
I-S-GAP quadrupole (135 at.)
I-S-GAP quadrupole (459 at.)
I-S-GAP quadrupole (1215 at.)
I-S-GAP cylinder (33633 at.)
FS cylinder (33633 at.)
DFT quadrupole (135 at.)
0.3
0.2
0.1
0
Energy [eV]
0
0.25
0.5
0.75
1.0
Reaction coordinate, r

GAP Results

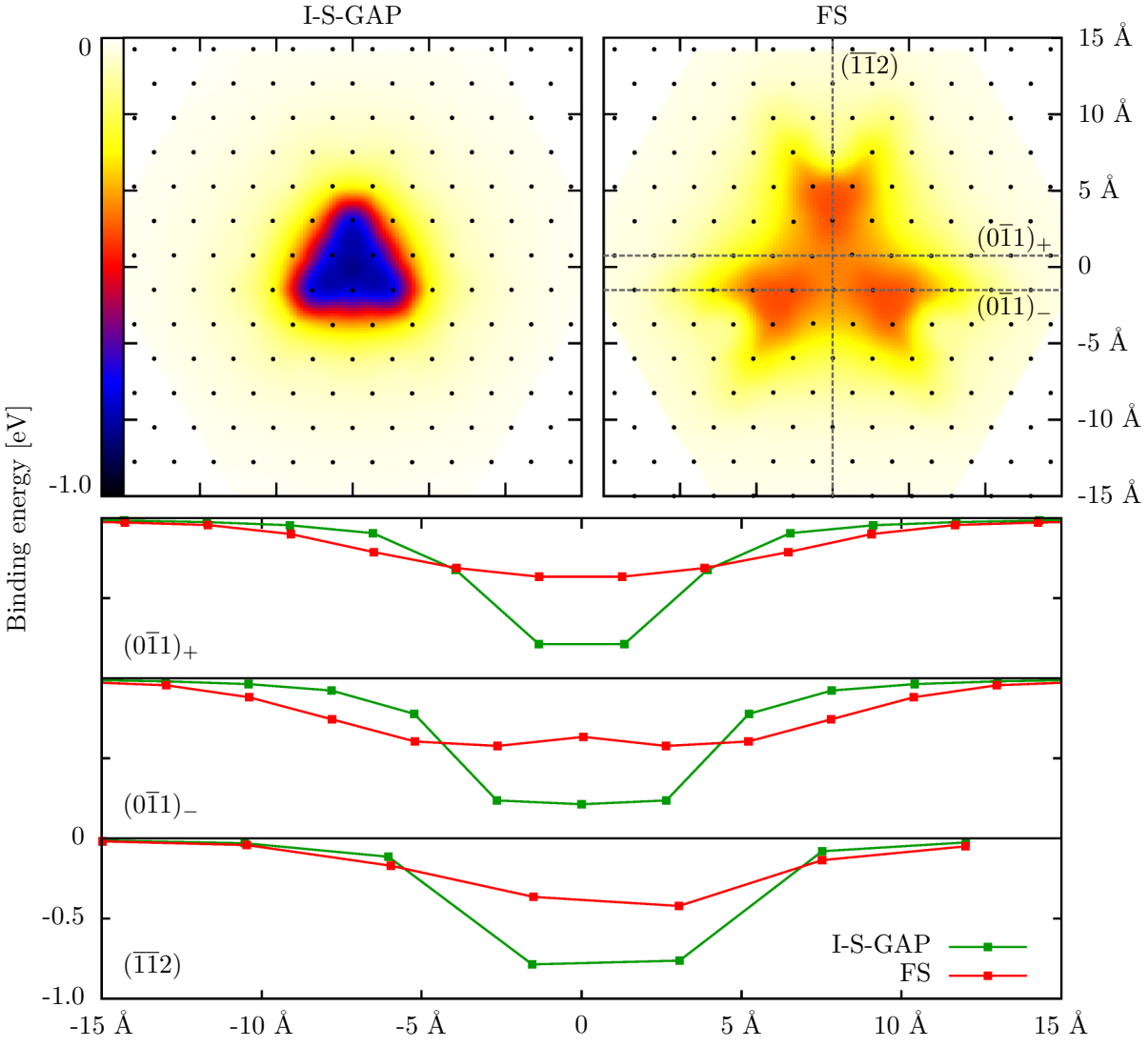
I-S-GAP
FS
0
-1.0
15 Å
10 Å
5 Å
0
-5 Å
-10 Å
-15 Å
$(\bar{1}\bar{1}2)$
$(0\bar{1}1)_+$
$(0\bar{1}1)_-$
Binding energy [eV]
$(0\bar{1}1)_+$
$(0\bar{1}1)_-$
$(\bar{1}\bar{1}2)$
0
-0.5
-1.0
I-S-GAP
FS
-15 Å
-10 Å
-5 Å
0
5 Å
10 Å
15 Å

Further Work

Tungsten Potential

- Crack propagation
- Dislocation jogs/kinks

Other Transition Metals

- Iron, iron + hydrogen
- Group 5 and 6 transition metals

Method Improvements

- Bond based smooth overlap of atomic positions
- Improvements to sparsification (dealing with large datasets)

Thank you for your attention.

Appendix

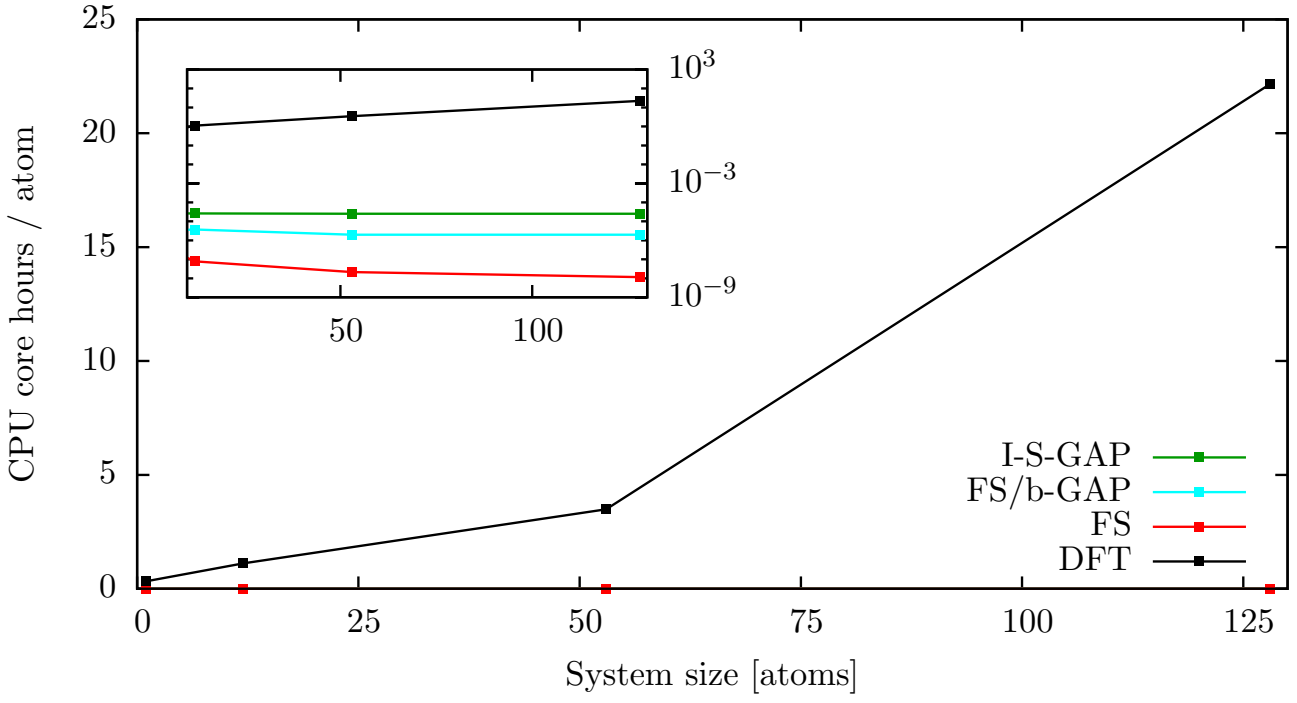
CPU core hours / atom
System size [atoms]
0
5
10
15
20
25
0
25
50
75
100
125
10^3
10^{-3}
10^{-9}
50
100
I-S-GAP
FS/b-GAP
FS
DFT

Appendix

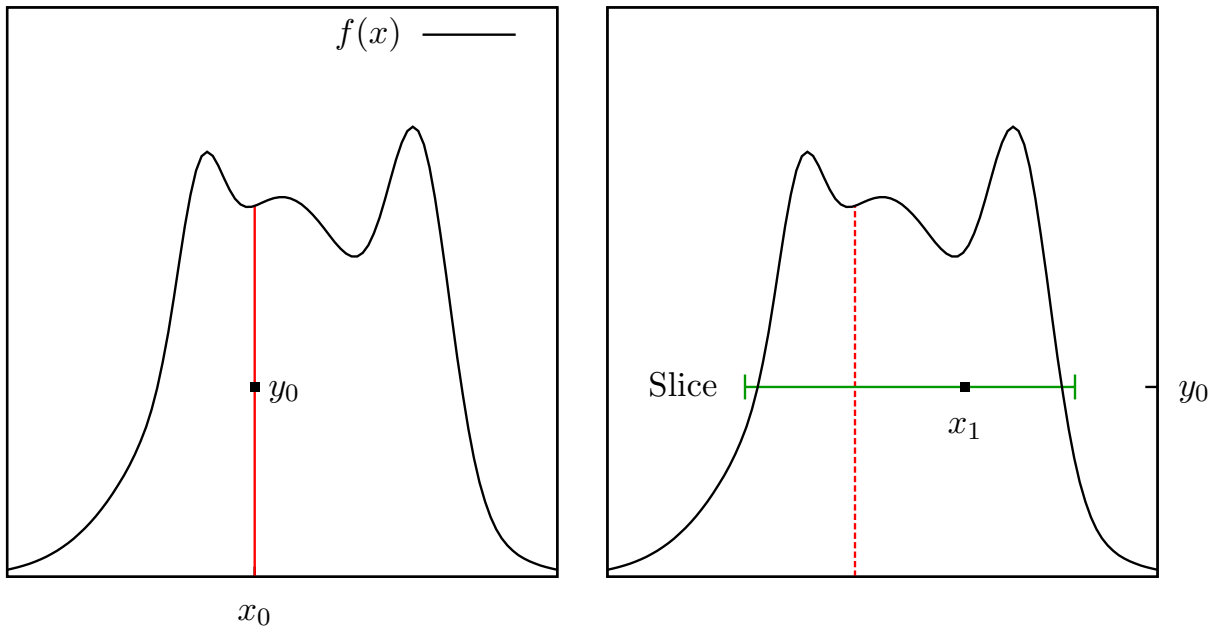

Appendix

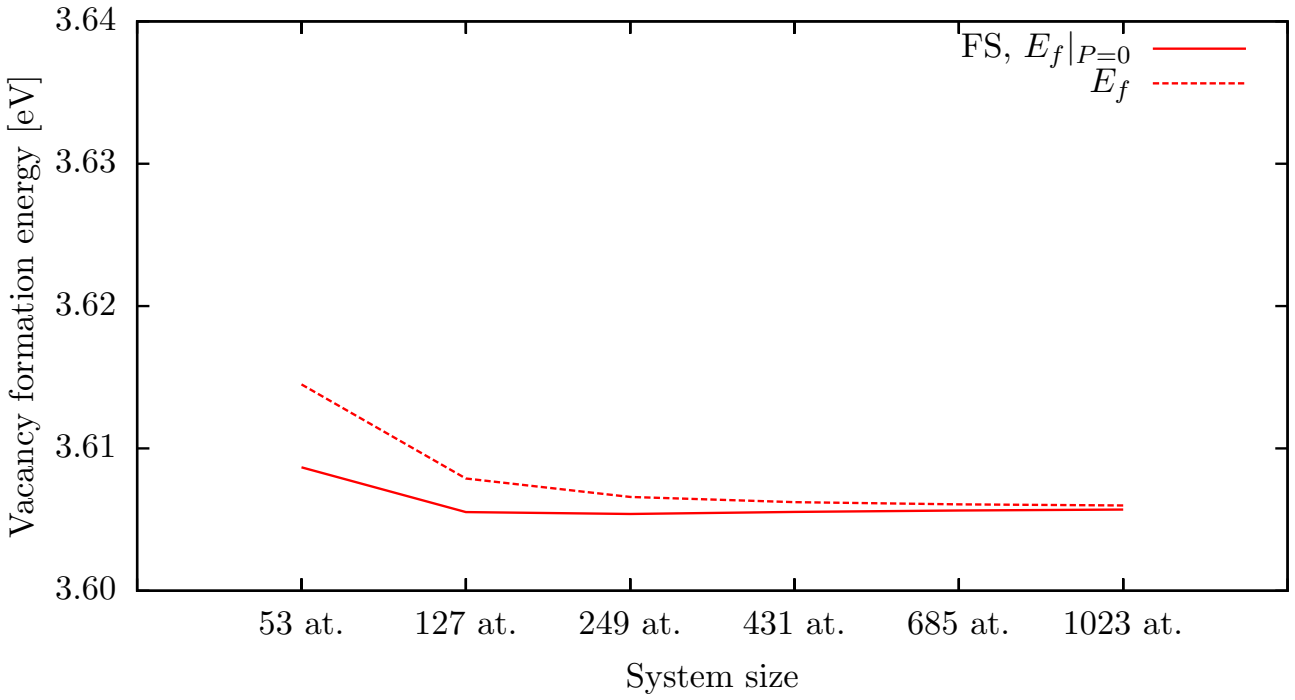
3.64
3.63
3.62
3.61
3.60
Vacancy formation energy [eV]
FS, $E_f|_{P=0}$
E_f
53 at.
127 at.
249 at.
431 at.
685 at.
1023 at.
System size

Appendix

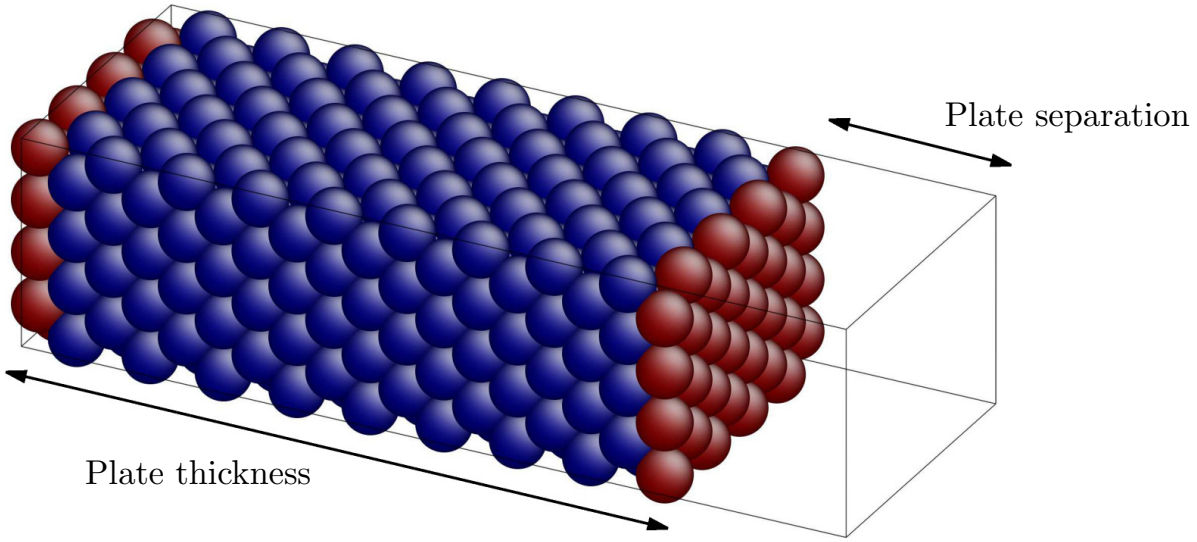

Appendix

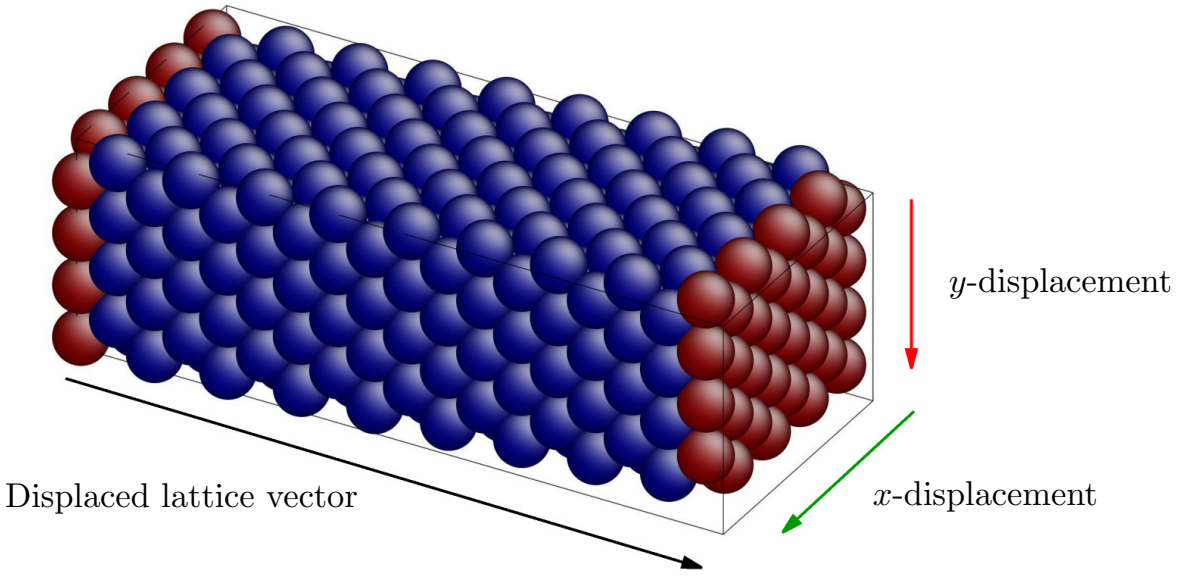

Appendix

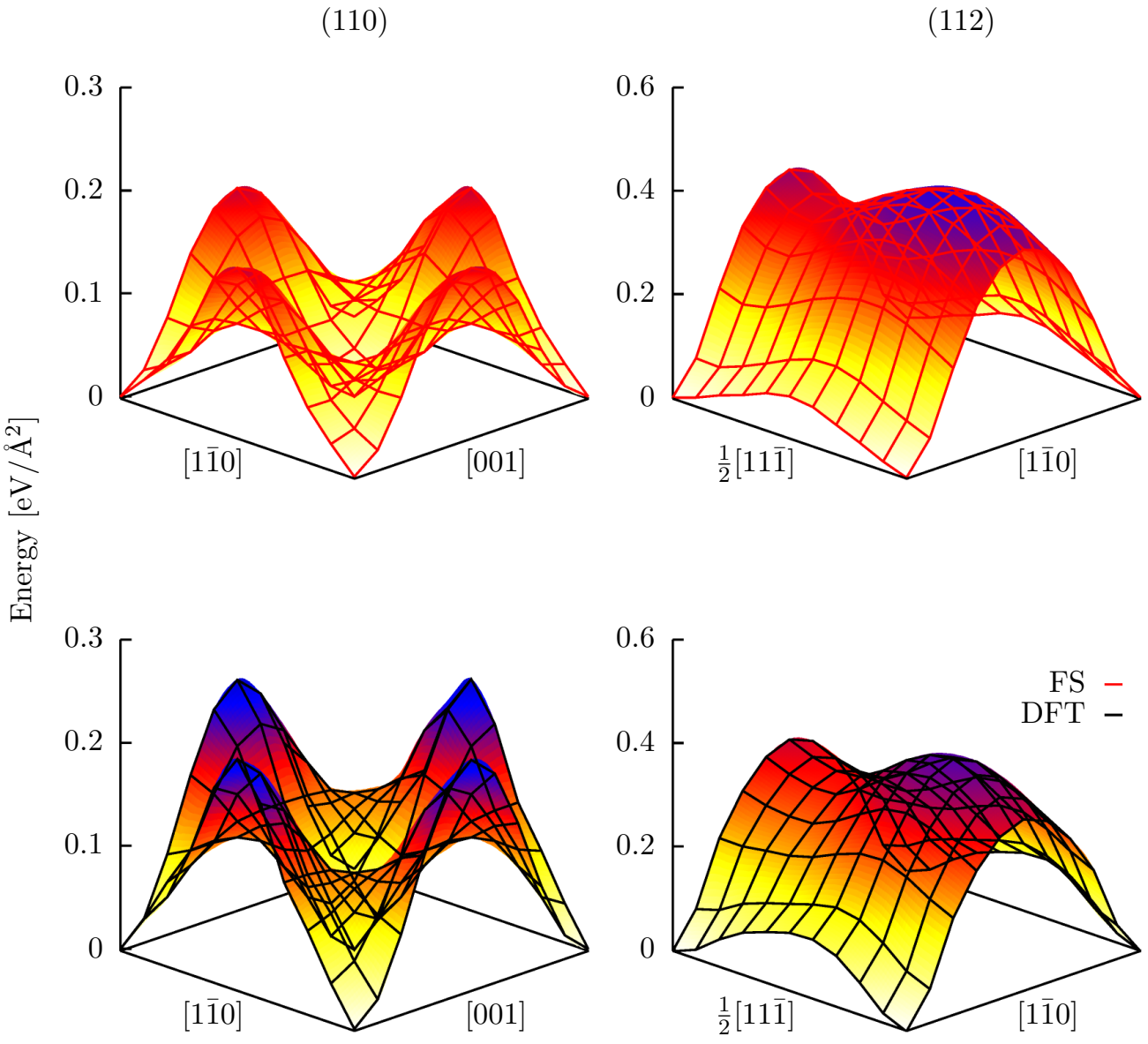
(110)
(112)
0.3
0.2
0.1
0
0.6
0.4
0.2
0
Energy [eV/Å^2]
[1$\bar{1}$0]
[001]
$\frac{1}{2}$[11$\bar{1}$]
[1$\bar{1}$0]
FS
DFT

Appendix

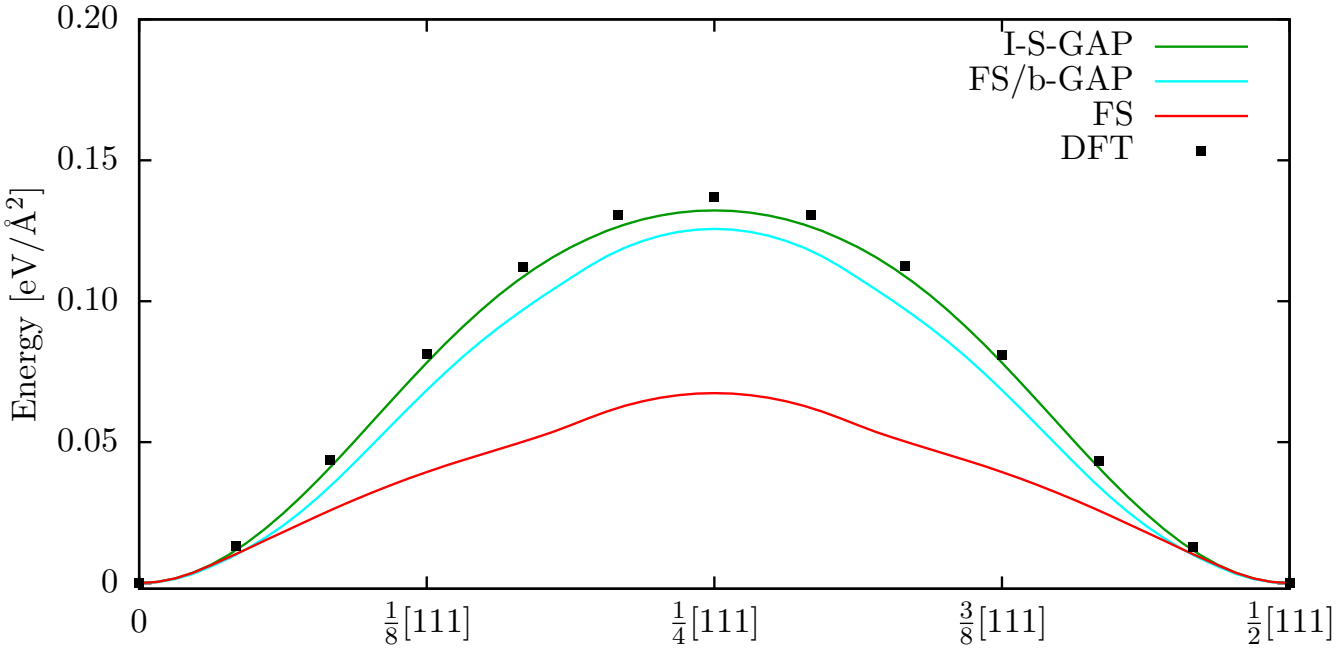
0.20
0.15
0.10
0.05
0
Energy [eV/Å^2]
0
$\frac{1}{8}$[111]
$\frac{1}{4}$[111]
$\frac{3}{8}$[111]
$\frac{1}{2}$[111]
I-S-GAP
FS/b-GAP
FS
DFT

Appendix

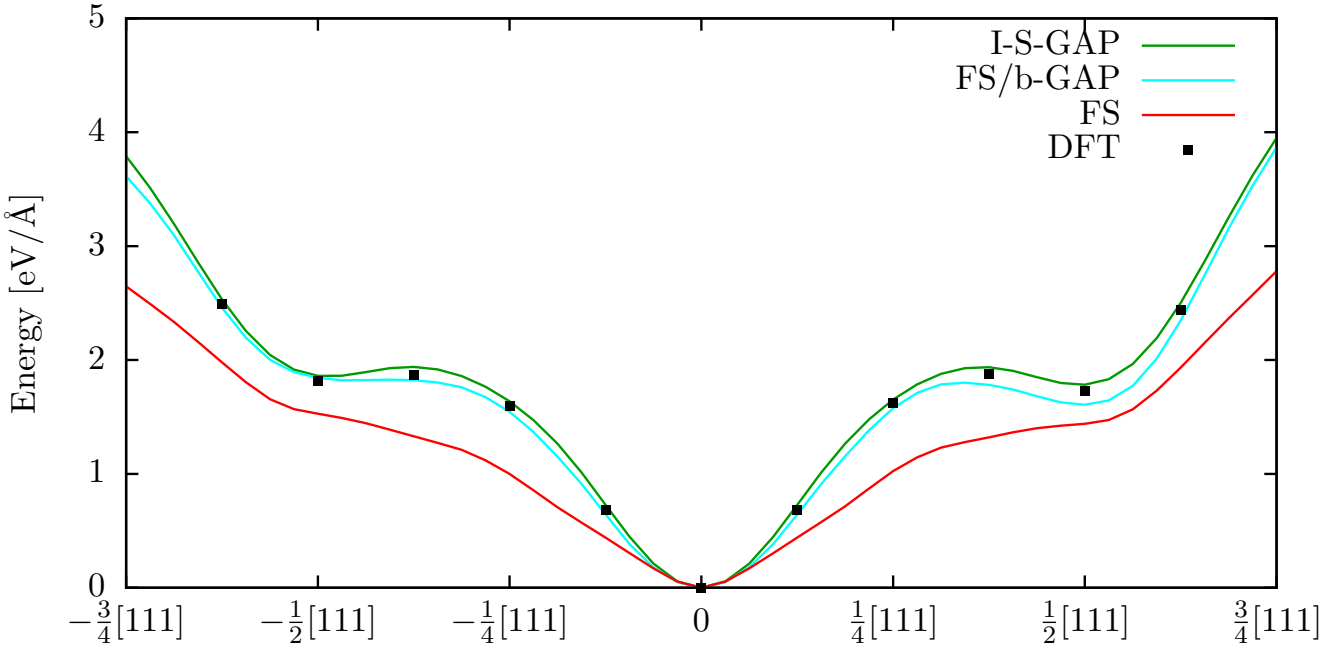
I-S-GAP
FS/b-GAP
FS
DFT
Energy [eV/Å]
5
4
3
2
1
0
$-\frac{3}{4}[111]$
$-\frac{1}{2}[111]$
$-\frac{1}{4}[111]$
0
$\frac{1}{4}[111]$
$\frac{1}{2}[111]$
$\frac{3}{4}[111]$

Appendix

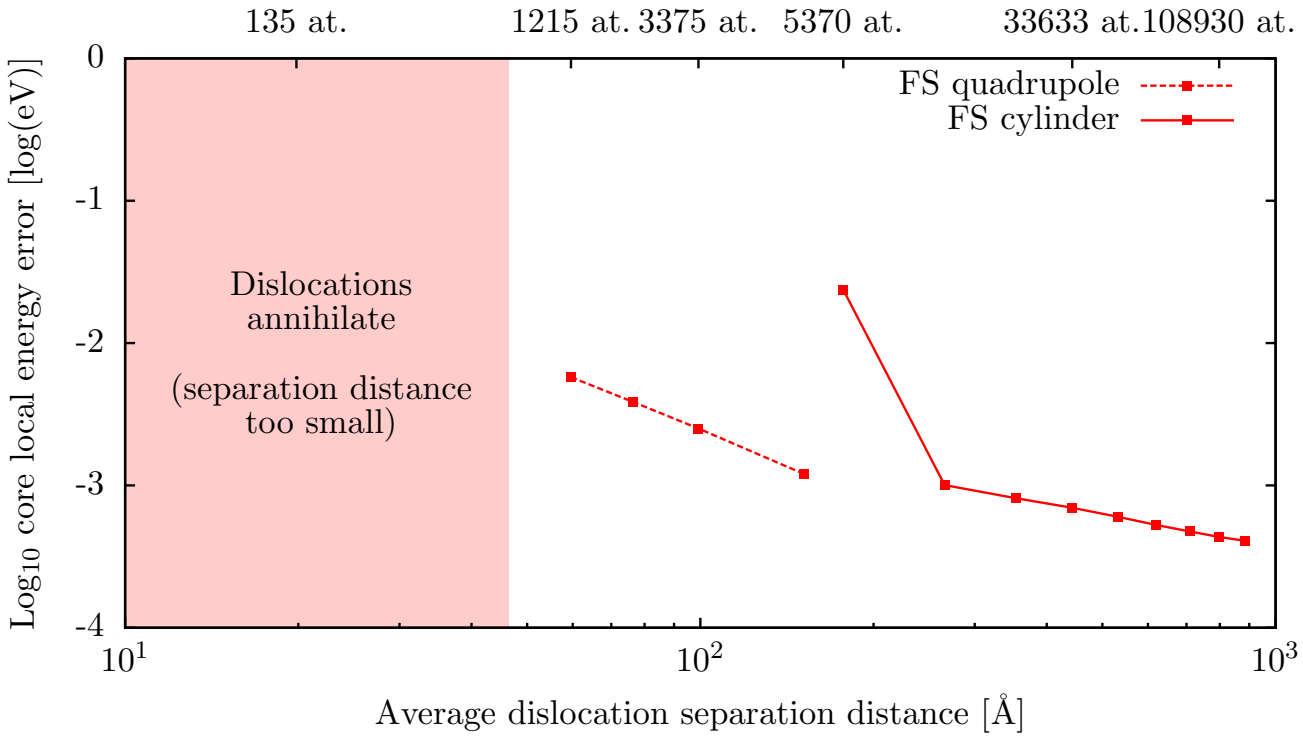
135 at.
1215 at.
3375 at.
5370 at.
33633 at.
108930 at.
FS quadrupole
FS cylinder
Dislocations annihilate
(separation distance too small)
Log10 core local energy error [log(eV)]
0
-1
-2
-3
-4
10^1
10^2
10^3
Average dislocation separation distance [Å]

Appendix

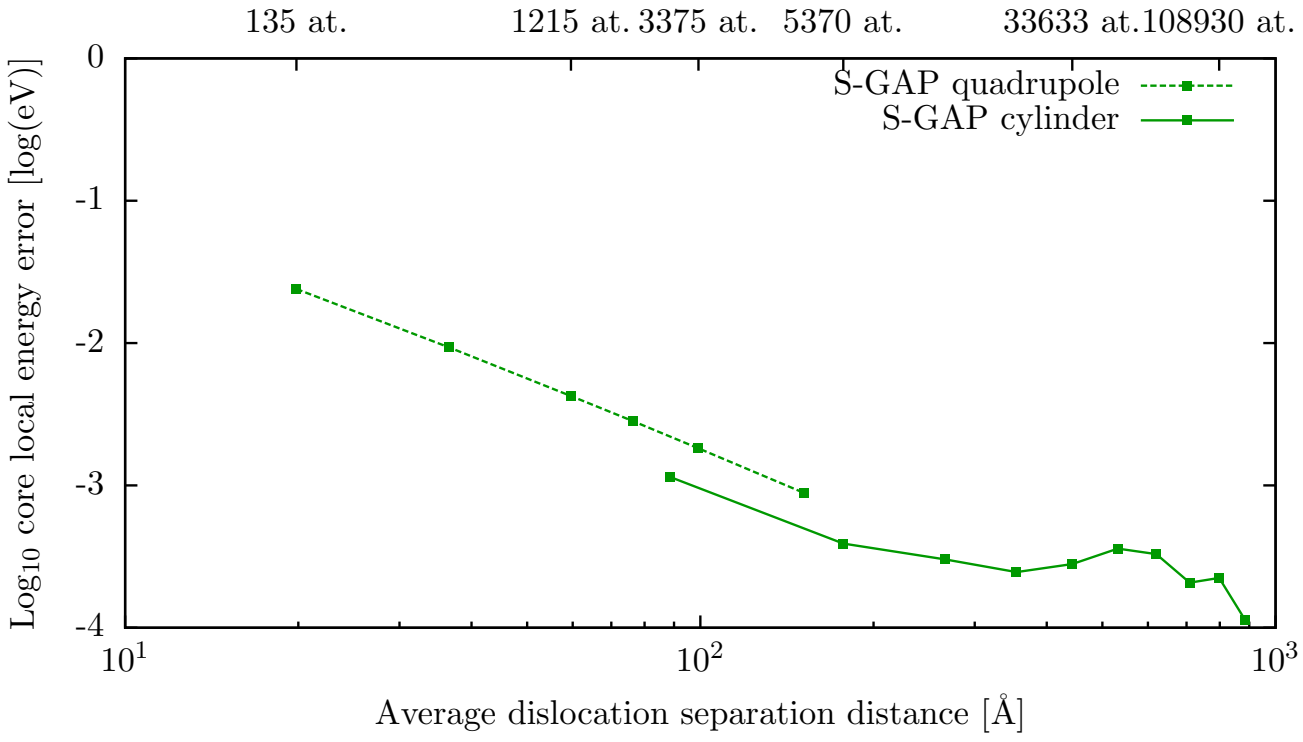
135 at.
1215 at.
3375 at.
5370 at.
33633 at.
108930 at.
S-GAP quadrupole
S-GAP cylinder
Log10 core local energy error [log(eV)]
0
-1
-2
-3
-4
10^1
10^2
10^3
Average dislocation separation distance [Å]

Appendix

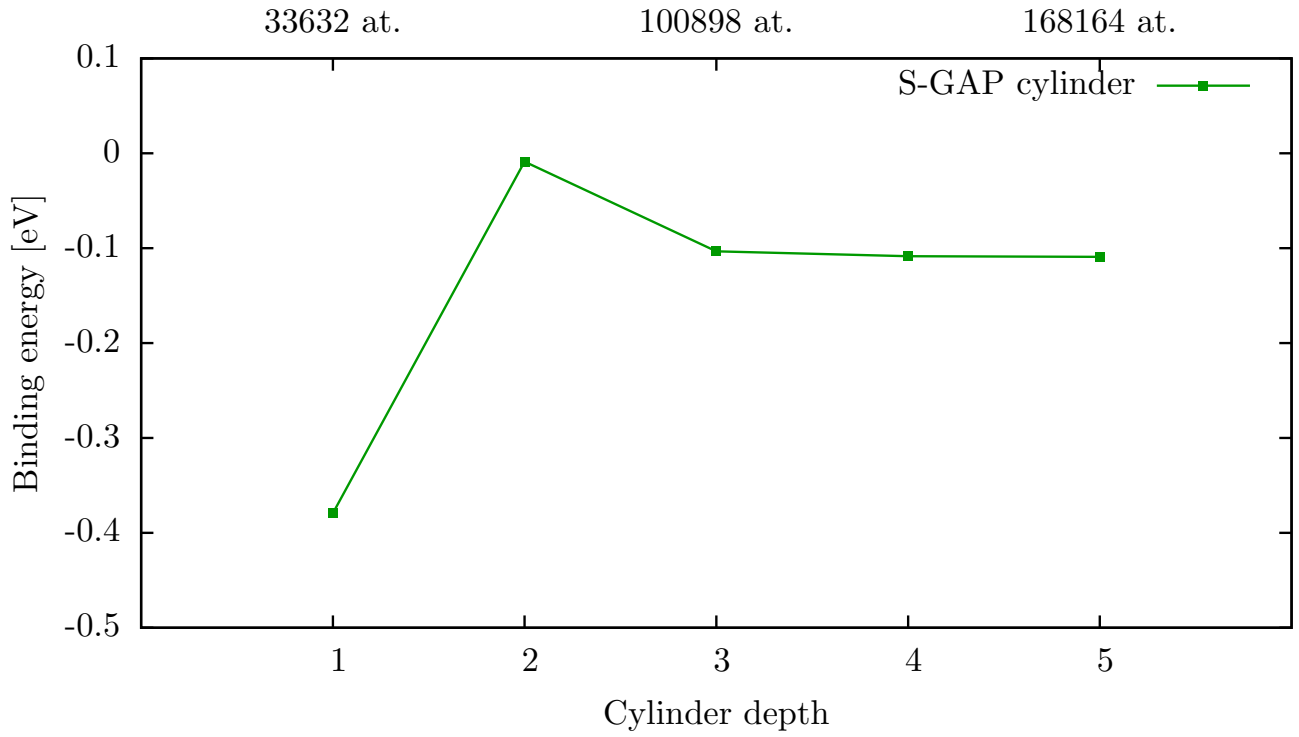
33632 at.
100898 at.
168164 at.
S-GAP cylinder
Binding energy [eV]
0.1
0
-0.1
-0.2
-0.3
-0.4
-0.5
1
2
3
4
5
Cylinder depth

Appendix